

A major purpose of the Technical Information Center is to provide the broadest dissemination possible of information contained in DOE's Research and Development Reports to business, industry, the academic community, and federal, state and local governments.

Although a small portion of this report is not reproducible, it is being made available to expedite the availability of information on the research discussed herein.

MASTER

Los Alamos National Laboratory is operated by the University of California for the United States Department of Energy under contract W-7405-ENG-36

LA-UR--86-2197

DE86 012436

JUL 07 1986

TITLE: SEARCH FOR RARE MUON AND PION DECAY MODES WITH THE
CRYSTAL BOX DETECTOR

AUTHOR(S): L. E. Pilonen, R. D. Bolton, J. D. Bowman, J. S. Frank,
A. L. Hallin, P. Heusi, C. M. Hoffman, G. E. Hogan, F. G. Mariam,
H. S. Matis, R. E. Mischke, D. E. Nagle, V. D. Sandberg,
G. H. Sanders, U. Sennhauser, R. Werbeck, R. A. Williams,
S. L. Wilson, R. Hofstadter, E. B. Hughes, M. Ritter, D. Grosnick,
S. C. Wright, V. L. Highland, and J. McDonough

SUBMITTED TO: Proceedings of the 2nd Conference on the Intersections Between
Particle and Nuclear Physics, Lake Louise, Canada,
May 26-31, 1986.

DISCLAIMER

This report was prepared as an account of work sponsored by an agency of the United States Government. Neither the United States Government nor any agency thereof, nor any of their employees, makes any warranty, express or implied, or assumes any legal liability or responsibility for the accuracy, completeness, or usefulness of any information, apparatus, product, or process disclosed, or represents that its use would not infringe privately owned rights. Reference herein to any specific commercial product, process, or service by trade name, trademark, manufacturer, or otherwise does not necessarily constitute or imply its endorsement, recommendation, or favoring by the United States Government or any agency thereof. The views and opinions of authors expressed herein do not necessarily state or reflect those of the United States Government or any agency thereof.

By acceptance of this article, the publisher recognizes that the U.S. Government retains a nonexclusive, royalty-free license to publish or reproduce the published form of this contribution, or to allow others to do so, for U.S. Government purposes.

The Los Alamos National Laboratory requests that the publisher identify this article as work performed under the auspices of the U.S. Department of Energy.

Los Alamos Los Alamos National Laboratory
Los Alamos, New Mexico 87545

JHF

SEARCH FOR RARE MUON AND PION DECAY MODES WITH THE CRYSTAL BOX DETECTOR

L.E. Piilonen, R.D. Bolton, J.D. Bowman, M.D. Cooper, J.S. Frank,
A.L. Hallin,^a P. Heusi,^b C.M. Hoffman, G.E. Hogan, F.G. Mariani,
H.S. Matis,^c R.E. Mischke,^d D.E. Nagle, V.D. Sandberg, G.H. Sanders,
U. Sennhauser,^d R. Verbeck, and R.A. Williams
Los Alamos National Laboratory, Los Alamos, New Mexico 87545

S.L. Wilson,^e R. Hofstadter, E.B. Hughes, and M. Ritter^f
Stanford University, Stanford, California 94305

D. Grosnick and S.C. Wright
University of Chicago, Chicago, Illinois 60637

V.L. Highland and J. McDonough
Temple University, Philadelphia, Pennsylvania 19122

ABSTRACT

New experimental upper limits for the branching ratios of the lepton-family-number nonconserving decays $\mu^+ \rightarrow e^+ \gamma$ and $\mu^+ \rightarrow e^+ \gamma \gamma$ are presented. A new determination of r , the ratio of pion axial vector to vector form factors, from radiative pion decay is also reported. These results are from data taken with the Crystal Box detector at LAMPF.

1. RARE MUON DECAYS

No process violating conservation of lepton family number, like $\mu^+ \rightarrow e^+ \gamma$, $\mu^+ \rightarrow e^+ e^+ e^-$, $\mu \rightarrow e^+ \gamma \gamma$, and $\mu^- A \rightarrow e^- A$, has ever been seen. Such processes are forbidden in the standard model¹ of electroweak interactions, but are allowed in many extensions to this model.² The existing experimental upper limits for the transition rates impose model-dependent constraints on the theoretical parameters, like mixing angles or gauge-boson masses, that describe such processes.

The best present experimental upper limits (90% C.L.) of the branching ratios for $\mu^+ \rightarrow e^+ \gamma$ and $\mu^+ \rightarrow e^+ \gamma \gamma$ are^{3,4}

$$B_{e\gamma} = \frac{\Gamma(\mu \rightarrow e\gamma)}{\Gamma(\mu \rightarrow \text{all})} \leq 1.7 \times 10^{-10} \quad \text{and} \quad B_{e\gamma\gamma} = \frac{\Gamma(\mu \rightarrow e\gamma\gamma)}{\Gamma(\mu \rightarrow \text{all})} \leq 8.4 \times 10^{-9}.$$

We report here improved limits for $B_{e\gamma}$ and $B_{e\gamma\gamma}$ from data taken with the Crystal Box detector in the stopped muon channel at the Clinton P. Anderson Meson Physics Facility (LAMPF).

The Crystal Box detector,⁵ shown in Fig. 1, consists of 396 NaI(Tl) crystals, 36 plastic scintillation hodoscope counters, and a cylindrical 8-plane stereo drift chamber⁶ surrounding a thin planar polystyrene target where muons decay at rest. The position resolution of each wire is 330 μm . The NaI(Tl) position resolution is 4.7 cm. The NaI(Tl) energy resolution for positrons and photons is $\sim 7\%$. The timing resolution of the NaI(Tl) is 1.2 ns and of the scintillators is 0.29 ns. (All resolutions are FWHM.)

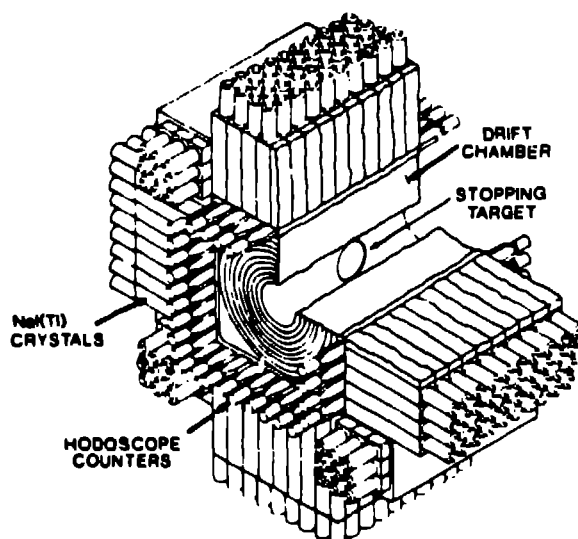


Fig. 1. The Crystal Box

The data for $\mu^+ \rightarrow e^+\gamma$, $\mu^+ \rightarrow e^+e^-e^-$, and $\mu^+ \rightarrow e^+\gamma\gamma$ were collected concurrently. Data written on magnetic tape for each candidate rare-decay event included timing and energy information from all hodoscope counters and from those NaI(Tl) crystals with at least 0.1 MeV deposited energy, and timing information from the drift-chamber cells that were hit.

The apparatus acceptances for the rare decay modes was determined with a Monte Carlo simulation, based on the shower code EGS3,⁷ that accurately reproduced the response of the detector to photons, positrons, and electrons.

The $\mu^+ \rightarrow e^+\gamma$ data analysis is presented first. The signature for a $\mu^+ \rightarrow e^+\gamma$ decay at rest is a positron and a photon back-to-back, in time coincidence, with $E_e = E_\gamma = 52.8$ MeV. The hardware trigger for $\mu^+ \rightarrow e^+\gamma$ required a coincidence within ± 5 ns of a "positron quadrant" and an opposite "photon quadrant", with at least 30 MeV deposited in the NaI(Tl) of each quadrant. A positron quadrant had a hodoscope counter signal and one or more NaI(Tl) discriminator signals. A photon quadrant had no hodoscope counter signal and at least one NaI(Tl) discriminator signal. The trigger selected $\sim 10^7$ candidate from $\sim 10^{12}$ muon decays. The detector resolutions for energies, times, and directions were sufficient to identify backgrounds from $\mu^+ \rightarrow e^+\nu\bar{\nu}\gamma$ and random coincidences.

The offline data reduction retained for subsequent analysis all $\mu^+ \rightarrow e\gamma$ events and an appreciable number of $\mu^+ \rightarrow e^+\nu\bar{\nu}\gamma$ events and random coincidences. The remaining 17 073 events satisfied $|\Delta t_{e\gamma}| < 5$ ns, $\theta_{e\gamma} \geq 160^\circ$, $E_e \geq 44$ MeV, and $E_\gamma \geq 40$ MeV. Fig. 2a shows $\Delta t_{e\gamma}$, the photon-positron relative timing, for a subset of these events. The broad distribution is due to random coincidences, while the prompt peak is due to $\mu^+ \rightarrow e^+\nu\bar{\nu}\gamma$ and possibly $\mu^+ \rightarrow e^+\gamma$.

The $\mu^+ \rightarrow e^+\gamma$ content was found by maximizing the likelihood

$$L(n_{e\gamma}, n_{IB}) = \prod_{i=1}^N \left[\frac{n_{e\gamma}}{N} P(\vec{x}_i) + \frac{n_{IB}}{N} Q(\vec{x}_i) + \frac{n_R}{N} R(\vec{x}_i) \right]$$

with respect to the parameters $n_{e\gamma}$, n_{IB} , and $n_R = N - n_{e\gamma} - n_{IB}$ that estimated the number of $\mu^+ \rightarrow e^+\gamma$, $\mu^+ \rightarrow e^+\nu\bar{\nu}\gamma$, and random events in the total sample of N events. P , Q , and R were the probability distributions for $\mu^+ \rightarrow e^+\gamma$, $\mu^+ \rightarrow e^+\nu\bar{\nu}\gamma$, and random events, respectively. The vector \vec{x} had components $\theta_{e\gamma}$, $\Delta t_{e\gamma}$, E_e , and E_γ .

Fig. 3 shows the normalized likelihood function. It peaks at $n_{e\gamma} = 0$ and $n_{IB} = 3470 \pm 80 \pm 300$ events. The latter agrees well

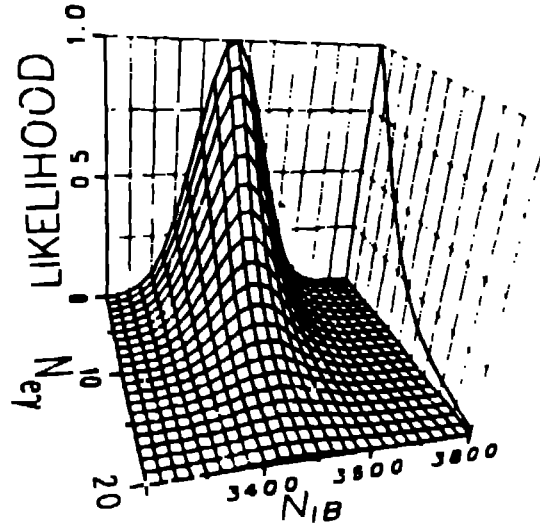
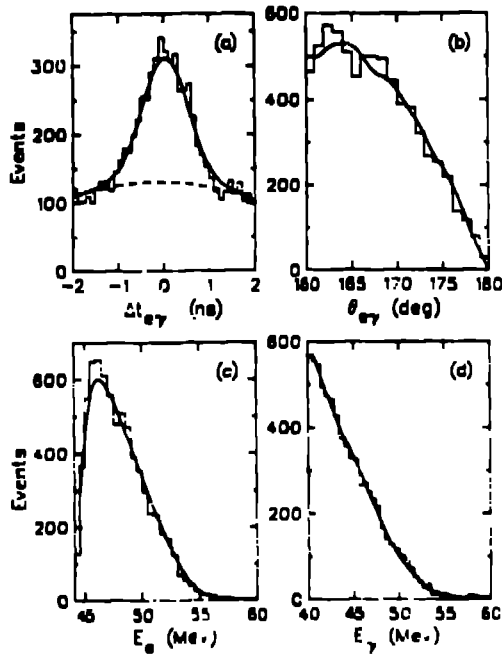


Fig. 2. Histograms of $e\gamma$ candidates Fig. 3. $\mu \rightarrow e\gamma$ likelihood

with the $3960 \pm 90 \pm 200 \mu^+ \rightarrow e^+ \nu \bar{\nu} \gamma$ events expected in the data. The likelihood function distribution implies $n_{e\gamma} < 11$ events (90% C.L.). Using the number of muons stopped, 1.35×10^{12} , during the live time of the experiment, the apparatus acceptance for $\mu^+ \rightarrow e^+ \gamma$, 0.305, and the detection efficiency, 0.545, we obtain $B_{e\gamma} < 4.9 \times 10^{-11}$. Fig. 2a-d shows the agreement between the data (histogrammed) and the best mix of $\mu^+ \rightarrow e^+ \nu \bar{\nu} \gamma$ and randoms (smooth) as determined by the likelihood analysis.

The preliminary analysis of ~ 60% of the $\mu^+ \rightarrow e^+ \gamma \gamma$ data is presented next. The signature for a $\mu^+ \rightarrow e^+ \gamma \gamma$ decay at rest is a positron and two photons in time coincidence emerging with zero net momentum and $E_{tot} = E_e + E_{\gamma 1} + E_{\gamma 2} = 105.6$ MeV. The three particles could strike two quadrants of the Crystal Box and fire the $e\gamma$ trigger discussed above, or could strike three quadrants and fire the $e\gamma\gamma$ trigger. The $\mu^+ \rightarrow e^+ \gamma \gamma$ trigger required a time coincidence within ± 5 ns of a positron quadrant and two photon quadrants, with at least 70 MeV deposited in the NaI(Tl) calorimeter.

The $e\gamma\gamma$ trigger recorded $\sim 10^6$ candidates from $\sim 10^{12}$ muon decays. In addition, $\sim 10^5$ candidates were found in the $e\gamma$ -triggered events, where the positron and one photon occupied the same quadrant. Fig. 4 shows the relative timing distribution for some of these events, the majority being backgrounds from triple random coincidences or two-particle prompt events in random coincidence with a third particle (e.g., $\mu^+ \rightarrow e^+ \nu \bar{\nu} \gamma + \gamma$).

The offline analysis removed most of the double- and triple-random coincidences while retaining all of the $\mu^+ \rightarrow e^+ \gamma \gamma$ events, assuming the most general local interaction for the

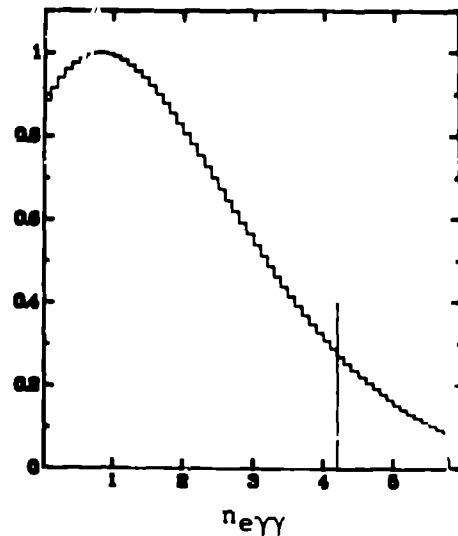
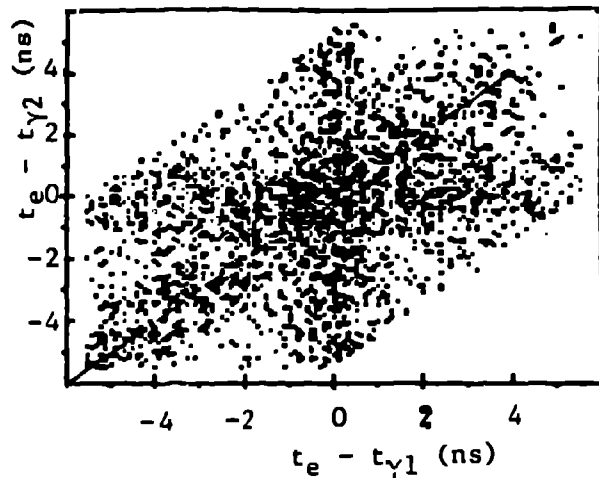


Fig. 4. Scatter plot of $e\gamma\gamma$ candidates Fig. 5. $\mu \rightarrow e\gamma\gamma$ likelihood

$\mu^+ \rightarrow e^+\gamma\gamma$ matrix element.⁸ Events with one particle showering and appearing as two hits in the trigger in coincidence with another particle were removed by energy and opening-angle cuts.

The number of $\mu^+ \rightarrow e^+\gamma\gamma$ events in the remaining sample of 15 events was estimated by maximizing the likelihood

$$L(n_{e\gamma\gamma}) = \prod_{i=1}^N \left[\frac{n_{e\gamma\gamma}}{N} P(\vec{x}_i) + \frac{n_R}{N} R(\vec{x}_i) \right]$$

with respect to the parameters $n_{e\gamma\gamma}$ and $n_R = N - n_{e\gamma\gamma}$ that estimated the number of $\mu^+ \rightarrow e^+\gamma\gamma$ and background events in the sample of N events. P and R were the probability distributions for $\mu^+ \rightarrow e^+\gamma\gamma$ and background, respectively. The components of \vec{x} were E_{tot} , $\Delta t = 2t_0 - t_{\gamma 1} - t_{\gamma 2}$, $p_{\parallel} = |\vec{p}_a + \vec{p}_b + \vec{p}_c \times \vec{p}_{ab}|$ and $\cos \alpha = \vec{p}_c \cdot \vec{p}_{ab}$, where \vec{p}_a and \vec{p}_b were the momenta most nearly perpendicular to each other, \vec{p}_{ab} was the unit vector normal to the \vec{p}_a - \vec{p}_b plane, and \vec{p}_c was the third particle's momentum.

The likelihood function distribution in Fig. 5 implies $n_{e\gamma\gamma} < 4.2$ (90% C.L.). Using the number of muons stopped, 8.5×10^{11} , during the live time of the experiment, the apparatus acceptance for $\mu^+ \rightarrow e^+\gamma\gamma$, 0.071, and the detector efficiency, 0.501, we obtain $B_{e\gamma\gamma} < 1.5 \times 10^{-10}$ (90% C.L.).

2. RADIATIVE PION DECAY

The low-energy behavior of QCD, the strong-interaction component of the standard model, is extremely difficult to determine. Nevertheless, there are serious attempts to calculate low-energy parameters such as the ratio $\gamma = F_A/F_V$ of the pion weak axial-vector to vector form factors. This ratio can be measured in the radiative decay of the pion, $\pi^+ \rightarrow e^+\nu_e\gamma$, where the decay rate is determined by the coherent admixture of an amplitude sensitive to

the strong interaction (γ dependent⁹) and an amplitude that accounts for QED corrections to the decay $\pi^+ \rightarrow e^+ \nu_e$.

The weighted averages of two previous measurements^{10,11} of γ are $\gamma = 0.41 \pm 0.06$ or $\gamma = -2.36 \pm 0.06$. The results are ambiguous because the experiments detected photons and positrons in a region of phase space where the term in the decay rate proportional to $(1+\gamma)^2$ dominates. We report here data that resolves the ambiguity in the measurement of γ .

Pions passed through a CH_2 degrader and a segmented scintillation beam counter, then stopped and decayed in a planar CH_2 target in the Crystal Box. The trigger required a coincidence within ± 5 ns of a positron quadrant and an opposite photon quadrant; these signals had to appear within 50 ns of a signal from the beam counters. The trigger recorded $\sim 10^7$ candidates from 4×10^{10} pion decays. Events from $\mu^+ \rightarrow e^+ \nu_e \gamma$ were eliminated by requiring $E_e + E_\gamma + |\vec{p}_e + \vec{p}_\gamma| > 115$ MeV. Events from $\pi^+ \rightarrow e^+ \nu_e \gamma$ and random coincidences in the shaded region of Fig. 6 with $105^\circ \leq \theta_{e\gamma} < 180^\circ$ were retained for subsequent analysis.

The ratio of the number of prompt events in the cross-hatched region of Fig. 6 to the number of pion stops (corrected for $\pi^+ \rightarrow e^+ \nu_e \gamma$ detection efficiency) gave the measured branching ratio for $\pi^+ \rightarrow e^+ \nu_e \gamma$ in this region. Comparing this measurement to the branching ratio calculated as a function of γ , we find $\gamma = 0.22 \pm 0.15$ or $\gamma = -2.13 \pm 0.15$, in agreement with the previous measurements.

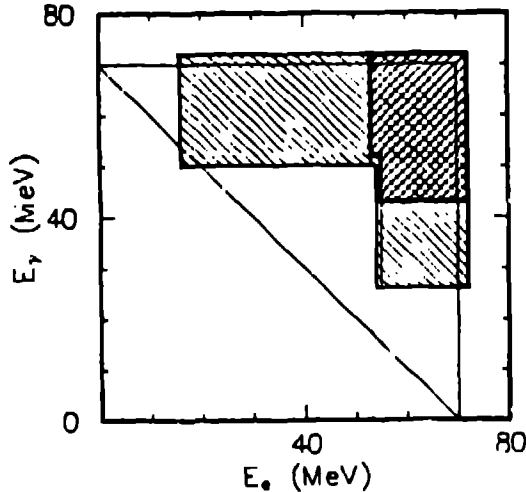


Fig. 6. $\pi^+ \rightarrow e^+ \nu_e \gamma$ Dalitz plot

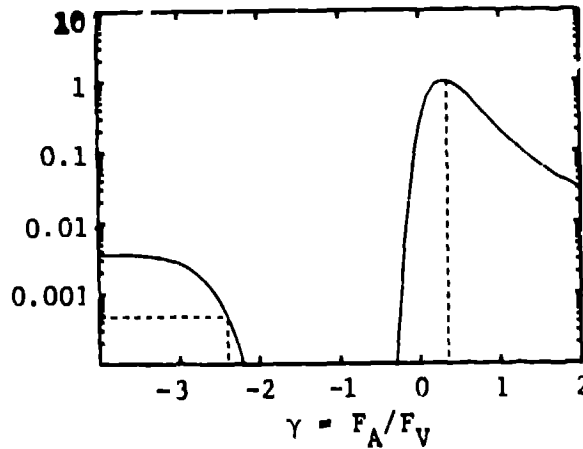


Fig. 7. $\pi^+ \rightarrow e^+ \nu_e \gamma$ likelihood

The distribution of events in the shaded region of Fig. 6 was used to resolve the ambiguity in γ . We maximized the likelihood

$$L(n_{e\nu\gamma}, \gamma) = \prod_{i=1}^N \left[\frac{n_{e\nu\gamma}}{N} P_\gamma(\vec{x}_i) + \frac{n_R}{N} R(\vec{x}_i) \right]$$

by varying the ratio γ and the parameters $n_{e\nu\gamma}$ and $n_R = N - n_{e\nu\gamma}$ that estimated of the number of $\pi^+ \rightarrow e^+ \nu_e \gamma$ and random events in the

sample of N events. P_γ and R were the probability distributions for $\pi^+ \rightarrow e^+ \nu_e \gamma$ (for a particular value of γ) and randoms, respectively. The coordinates of \vec{x} were $\theta_{e\gamma}$, $\Delta\theta_{e\gamma}$, E_e , and E_γ .

Fig. 8 shows the normalized likelihood as a function of γ . The positive value for γ is favored over the negative value by a likelihood ratio of 2175 to 1. Thus we obtain the unique solution $\gamma = 0.22 \pm 0.15$. The new world average is $\gamma = 0.38 \pm 0.06$.

3. SUMMARY

Using data from μ^+ decays in the Crystal Box detector, we have obtained improved upper limits on the branching ratios of the lepton-family-number nonconserving decays $\mu^+ \rightarrow e^+ \gamma$ and $\mu^+ \rightarrow e^+ \gamma \gamma$ of $B_{e\gamma} < 4.9 \times 10^{-11}$ and $B_{e\gamma\gamma} < 1.5 \times 10^{-10}$, respectively. Using data from π^+ decays, we have resolved the ambiguity in the measurement of γ , the ratio of pion axial-vector to vector form factors, in favor of the positive value, with a new world average of $\gamma = 0.38 \pm 0.06$.

We acknowledge the extraordinary assistance from the many people at each of our institutions and from the operations staff at LAMPF. This work was supported in part by the U.S. Department of Energy and the National Science Foundation.

REFERENCES

- a. Now at Physics Dept., Princeton University, Princeton, NJ 08544
 - b. Now at ELEKTROWATT Ing. AG., Zurich, Switzerland
 - c. Now at Lawrence Berkeley Laboratory, Berkeley, CA 94720
 - d. Now at SIN, CH-5234 Villigen, Switzerland
 - e. Now at Los Alamos National Laboratory, Los Alamos, NM 87545
 - f. Now at Lockheed Missiles and Space Company, Palo Alto, CA 94304
1. S.L. Glashow, Nucl. Phys. 22, 579 (1961); S. Weinberg, Phys. Rev. Lett. 19, 1264 (1967); A. Salam, in Elementary Particle Theory: Relativistic Groups and Analyticity (Nobel Symposium No. 8), ed. N. Svartholm (Almqvist and Wiksells, Stockholm, 1968), p. 367.
 2. C.M. Hoffman, in Fundamental Interactions in Low-Energy Systems, ed. P. Dalpiaz et al., (Plenum Press, New York, 1985), p. 138; P. Herczeg and T. Oka, Phys. Rev. D 29, 475 (1984); D.E. Nagle, Comments on Nuclear and Particle Physics XI, 277 (1983).
 3. W.W. Kinnison et al., Phys. Rev. D 25, 2846 (1982).
 4. G. Azuelos et al., Phys. Rev. Lett. 51, 164 (1983).
 5. R.D. Bolton et al., Phys. Rev. Lett. 56, 2461 (1986) and references therein.
 6. R.D. Bolton et al., Nucl. Instr. and Methods 241, 52 (1985).
 7. R.L. Ford and W.R. Nelson, Stanford Linear Accelerator Center No. SLAC-210, 1978 (unpublished).
 8. J.D. Bowman et al., Phys. Rev. Lett. 41, 442 (1978).
 9. D.A. Bryman et al., Phys. Rep. 88, 151 (1982).
 10. A. Stetz et al., Nucl. Phys. B 4, 189 (1978).
 11. A. Bay et al., Proceedings of Tenth International Conference on Particles and Nuclei, Heidelberg (1984).